



Rapid pressure-assisted sinter bonding in air using 200 nm Cu particles and enhancement of bonding strength by successive pressureless annealing

Myeong In KIM, Jong-Hyun LEE

Department of Materials Science and Engineering, Seoul National University of Science and Technology,
232 Gongneung-ro, Nowon-gu, Seoul 139-743, Korea

Received 2 March 2021; accepted 26 October 2021

Abstract: To design an effective and realistically applicable sinter bonding process for power devices, we proposed a two-step process using a 200 nm Cu-particle-based paste to form a bondline having high-temperature sustainability and superior thermal conductance. This process involved rapid pressure-assisted sinter bonding in air followed by pressureless annealing in a nitrogen atmosphere. In the case of a paste prepared with a mixture of 20 wt.% malic acid and 80 wt.% ethylene glycol, sinter bonding at 300 °C and 5 MPa for only 30 s resulted in a sufficient shear strength of 23.1 MPa. The shear strength was significantly enhanced to 69.6 MPa by the additional pressureless aging for 30 min. Therefore, the two-step sinter bonding process is expected to provide an outstanding production rate as a next-generation sinter bonding process.

Key words: submicron Cu particles; Cu paste; malic acid; sinter bonding; successive annealing; shear strength

1 Introduction

To achieve a bondline with both high-temperature sustainability and high thermal conductivity in the mounting of wide bandgap devices for next-generation power modules [1,2], sinter bonding techniques using pastes containing silver (Ag) or copper (Cu) particles have been studied extensively. For example, WANG et al [3] obtained a shear strength of ~50 MPa in a bondline formed by pressureless sinter bonding for 10 min at 250 °C in air using a paste containing 600 nm Ag particles and optimal Ag surface finish roughness. Furthermore, PENG et al [4] reported a shear strength exceeding 30 MPa in a bondline formed by pressure (2 MPa)-assisted sinter bonding for 5 min at 200 °C in argon (Ar) using a paste containing micro-nano Cu composite particles and Cu surface finishes. Although this bonding technique requires a

significantly low bonding temperature, the bonding time is inevitably long because sintering is accomplished in the solid state. Moreover, current studies on sinter bonding have mainly focused on the use of less expensive Cu particles.

Although the thermal and electrical conductivities of Cu are similar to those of Ag, Cu is significantly susceptible to oxidation in air [5]. ZUO et al [6] reported that the oxidation of Cu particles results in the formation of copper oxide as tiny protrusions on the surface, and the oxide makes sintering difficult by interrupting diffusion paths. Therefore, early sinter bonding studies using Cu particles were carried out under a reduced atmosphere. For example, ISHIZAKI and WATANABE [7] performed pressure (5 MPa)-assisted sinter bonding using 20 nm Cu nanoparticles under a hydrogen atmosphere. Since then, others such as PENG et al [4], LIU et al [8], and GAO et al [9] also attempted sinter bonding

under an inert atmosphere. However, considering the existence of native copper oxide, the use of a paste with self-reducing properties is necessary. For example, MOU et al [10] demonstrated the significance of the self-reducibility of a paste containing isopropanolamine in the sinter bonding of 6.5 nm Cu nanoparticles for 30 min in Ar under 5 MPa compression. ZUO et al [6] obtained a shear strength exceeding 30 MPa after sinter bonding for 5 min with a Cu paste containing 50 nm Cu nanoparticles and glycerol under 3 MPa compression. However, from the viewpoint of shortening the bonding time, the solid-state sintering under moderate compression still requires a long bonding time beyond the time that can be dedicated to a mass production line.

In the present study, a two-step sinter bonding process suitable for a mass production line was designed, and its feasibility was evaluated. This process involves a rapid pressure-assisted sinter bonding step and a subsequent pressureless annealing step. This concept can be realized on a conveyor line by adding a buffer line between the two steps and provides a continuous manufacturing method for mass production.

To achieve rapid bonding under compression, the adoption of small Cu particles is essential. Thus, Cu nanoparticle-based pastes have been used in most Cu-based sinter bonding experiments. For instance, ZUO et al [11] used 20 nm Cu nanoparticles for a pressure (4 MPa)-assisted sinter bonding process over 5 min at 250 °C. MOU et al [12] adopted smaller Cu nanoparticles (6.5 nm) for pressure (2 MPa)-assisted sinter bonding over 10 min at 250 °C. However, the use of very small nanoparticles poses a practical challenge in terms of ensuring a uniform dispersion of particles in the mass production of the paste. Therefore, in this study, 200 nm Cu particles were chosen to satisfy both the high-speed sinter bonding and the production of the homogeneous paste. Moreover, a high-boiling polyol was used as the solvent for the preparation of the sintering paste. This solvent can suppress the oxidation of Cu particles by air during heating to 300 °C and reduce the Cu₂O surface on the Cu particle near the peak sintering temperature [13].

Meanwhile, because the self-reduction potential in a paste containing Cu particles is a crucial factor for the in situ reduction-sintering of

the particles, the addition of additives for the reduction may also be considered. Among the studies on additives, a carboxylic acid added to a paste or an ink containing Cu particles has been reported to be useful for reducing the existing copper oxide. KANZAKI et al [14] achieved a low resistivity of $5.5 \times 10^{-5} \Omega \cdot \text{cm}$ after sintering Cu ink in air at 150 °C for 10 s; the Cu ink was prepared by the addition of different carboxylic acids to a solvent mixture of propylene glycol and glycerol. MOU et al [15] increased the shear strength from 6.8 to 20.2–32.4 MPa with the addition of 3% of a carboxylic acid to a paste comprising 60 nm Cu nanoparticles and dehydrated ethanol through pressure (10 MPa)-assisted sinter bonding in an Ar–5% H_2 mixture at 250 °C for 60 min. Hence, a selected carboxylic acid (malic acid (MA)) was added to the paste used in this study to remove the copper oxide in the Cu particles more effectively.

2 Experimental

2.1 Materials

The Cu particles were synthesized in the laboratory by a modified polyol synthesis method through heating after complete dissolving of the Cu precursor and surfactant in a polyol solvent. The prepared particles were mixed with ethylene glycol (EG, C₂H₆O₂, 99.98%, LG Chemical) at a particle-to-solvent mass ratio of 83:17 using a spatula to prepare a reference paste, which was named EG paste. Further, another paste was prepared by manually mixing an EG solution of MA and Cu particles. The MA solution was prepared by dissolving 10–20 wt.% MA (C₄H₆O₅, ≥99%, Sigma-Aldrich) in EG at 60 °C. The main paste was named the EG–20wt.%MA paste.

2.2 Sinter bonding

Chip sinter bonding was performed with a dummy Cu die with sizes of 3 mm × 3 mm and a dummy Cu substrate with sizes of 10 mm × 10 mm. To remove the surface oxide, both the die and substrate were polished with 2000 grit sandpaper and then immersed in a 10% H₂SO₄ solution for 1 min. Hence, the initial surfaces of the die and substrate were expected to be primarily covered by the native oxide.

The prepared Cu paste was preferentially stencil-printed onto the substrate through a stencil

mask with a slit of 3 mm × 3 mm × 0.1 mm. Subsequently, the die was placed on the printed pattern with alignment, and the sandwich-structured sample was placed and heated on a chuck at 300 °C. Immediately after placement, a collet heated to an identical temperature pressed the center of the chip, after which the bonding time was recorded. To ensure compatibility with the real mass production, sinter bonding in air was performed for only 30 s with the assistance of 2–5 MPa pressure throughout the bonding process. After pressure-assisted bonding, pressureless annealing was conducted at 300 °C for 10–30 min in a nitrogen-containing chamber to strengthen the sinter bonding.

2.3 Characterization

The initial morphologies of the used Cu particles, the cross-sectional microstructures of the bondlines after bonding, and the fracture surfaces after the shear tests were observed using a high-resolution scanning electron microscope (HR-SEM; SU8010, Hitachi). Images of the bondline interface were obtained in the backscattered electron (BSE) mode. The thermal behaviors of the substances and pastes in air were examined by thermogravimetric and differential thermal analysis (TG-DTA, DTG-60, Shimadzu) at a heating rate of 20 °C/min. The bonding strength of the bondline was measured by shearing using a Dage-4000 tester (Nordson DAGE). The shear strength is defined as the maximum stress measured during shearing (speed of 200 μm/s) at the height of 200 μm from the surface of the substrate.

3 Results and discussion

3.1 Morphology of Cu particles

Figure 1 shows the morphology of the synthesized Cu particles used as fillers. They had an average size of 192 nm, and their size distribution ranged from 120 to 300 nm. The D_{50} value was 188 nm. Furthermore, the aggregation of particles was not severe, considering the particle size. Although most of the particles were irregular, particles of various polygonal shapes with smooth surfaces were also found.

3.2 Microstructures of bondlines

The shear strength measured immediately after sinter bonding at 5 MPa for only 30 s at 300 °C

was 6.7 and 23.1 MPa for the EG paste and EG-20wt.%MA paste, respectively. The achieved shear strength of 23.1 MPa surpassed that reported for bonding obtained using the current high-temperature solder of Pb-5Sn [16].

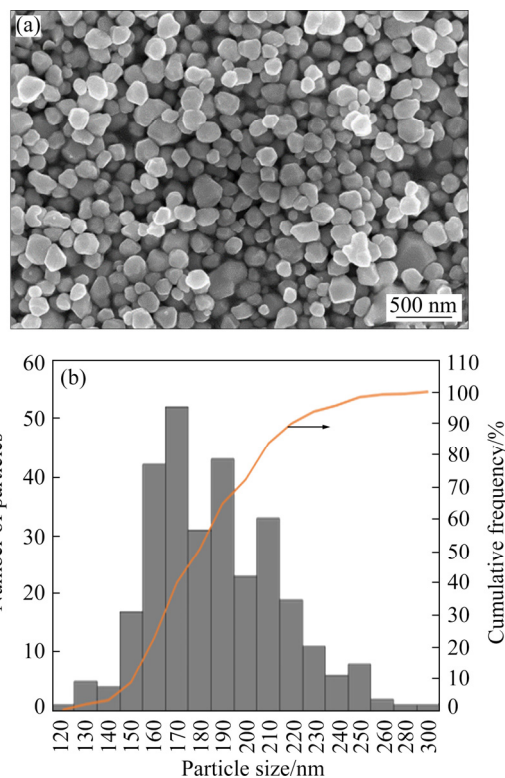


Fig. 1 SEM image (a) and size histogram of synthesized copper particles (b)

The large difference in the strength suggests that there are obvious differences in the sinter bonding state and mechanism. Figure 2 shows the bondline microstructures formed immediately after sintering for 30 s at 300 °C for the two pastes. The microstructures of the two bondlines immediately after pressure-assisted sinter bonding were observed to be uniformly porous (Figs. 2(a, d)). In addition, the Cu particles in the paste were sintered in parts with Cu finishes at the upper and lower interfaces, as shown in Figs. 2(b, c, e, f). However, the number of Cu particles participated during the sintering was clearly lower in the case of the paste containing only EG solvent compared to that of the EG-20wt.%MA paste, as shown in Figs. 2(b, c, e, f). As a result, a larger number of tiny interparticulate voids were observed in the bondline formed using the EG paste, although slightly larger voids existing between locally sintered regions were observed in the EG-20wt.%MA paste. In Figs. 2(a) and (d) images,

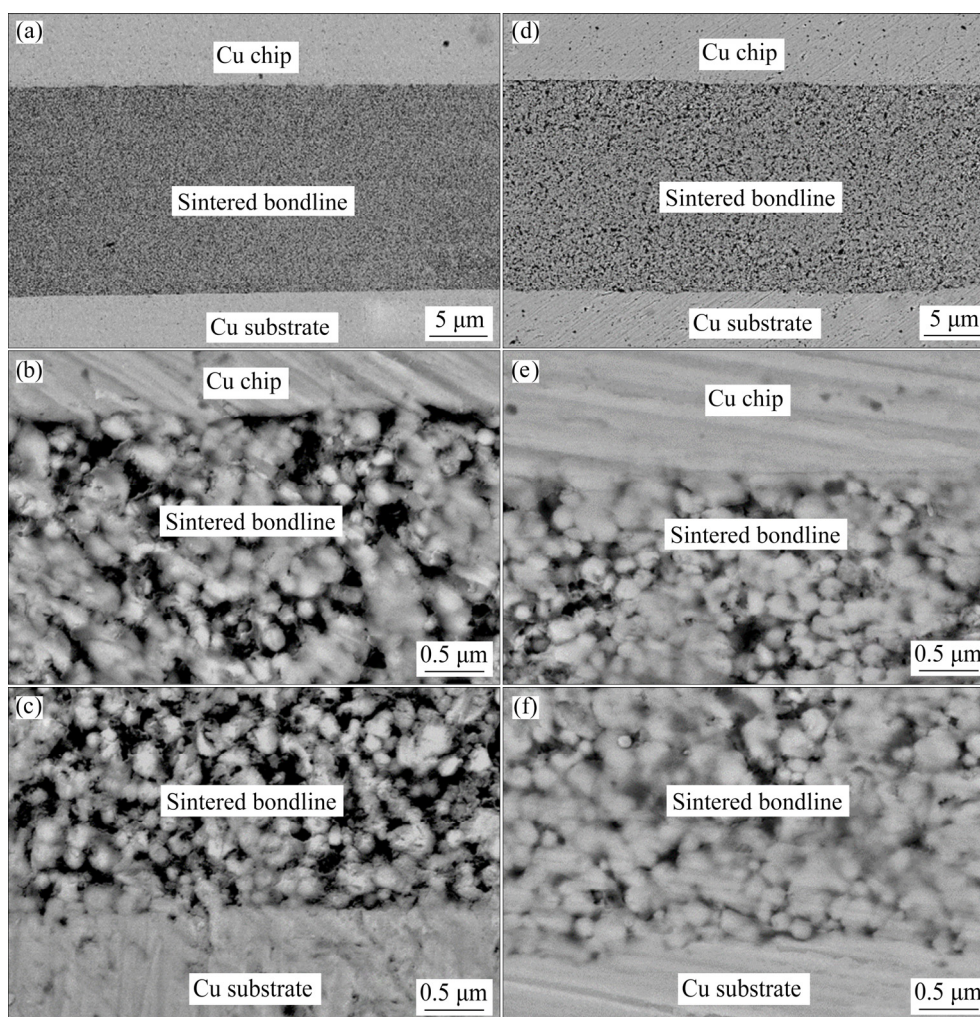


Fig. 2 Cross-sectional bondline BSE images of samples sinter-bonded at 5 MPa and 300 °C for 30 s in air using EG paste (a–c) and EG–20wt.%MA paste (d–f): (a, d) Low-magnification images revealing overall bondline; (b, c, e, f) Magnified images of upper (b, e) and lower (c, f) interfaces

the porosities measured using self-produced image analysis software were 13.9% and 11.0%, respectively. The enhanced degree of sintering in the bondline formed using the EG–20wt.%MA may account for the significant improvement in the shear strength, indicating that the added MA eliminates the surface oxide layer of Cu particles and thus aids the sintering of Cu particles.

3.3 TG–DTA results for pastes

The cause of the enhanced sintering in the paste containing MA was analyzed by thermogravimetric and differential thermal analysis (TG–DTA) measurements, and the data are displayed in Fig. 3. EG evaporated in the range of 50–170 °C with an endothermic peak at 159 °C (Fig. 3(a)), while MA evaporated at 180–270 °C

with an endothermic peak at 262 °C (Fig. 3(b)). Thus, the evaporation of solvents in the EG–20wt.%MA mixture started at 50 °C but lasted up to temperatures exceeding 400 °C (Fig. 3(c)). In case of the EG paste (Fig. 3(d)), however, evaporation occurred preferentially, followed by mass increase behavior with an exothermic peak at 198 °C. Considering the lower mass decrease from 156 °C onwards and the mass increase/appearance of an exothermic peak from 198 °C onwards, it was inferred that the Cu particles in the EG paste started to undergo oxidation from 156 °C onwards and underwent severe oxidation when the temperature exceeded 198 °C. Lastly, the mass increase caused by the oxidation of Cu in the EG–20wt.%MA paste started at 299 °C Fig. 3(e). However, the peak temperatures of the two exothermic peaks observed

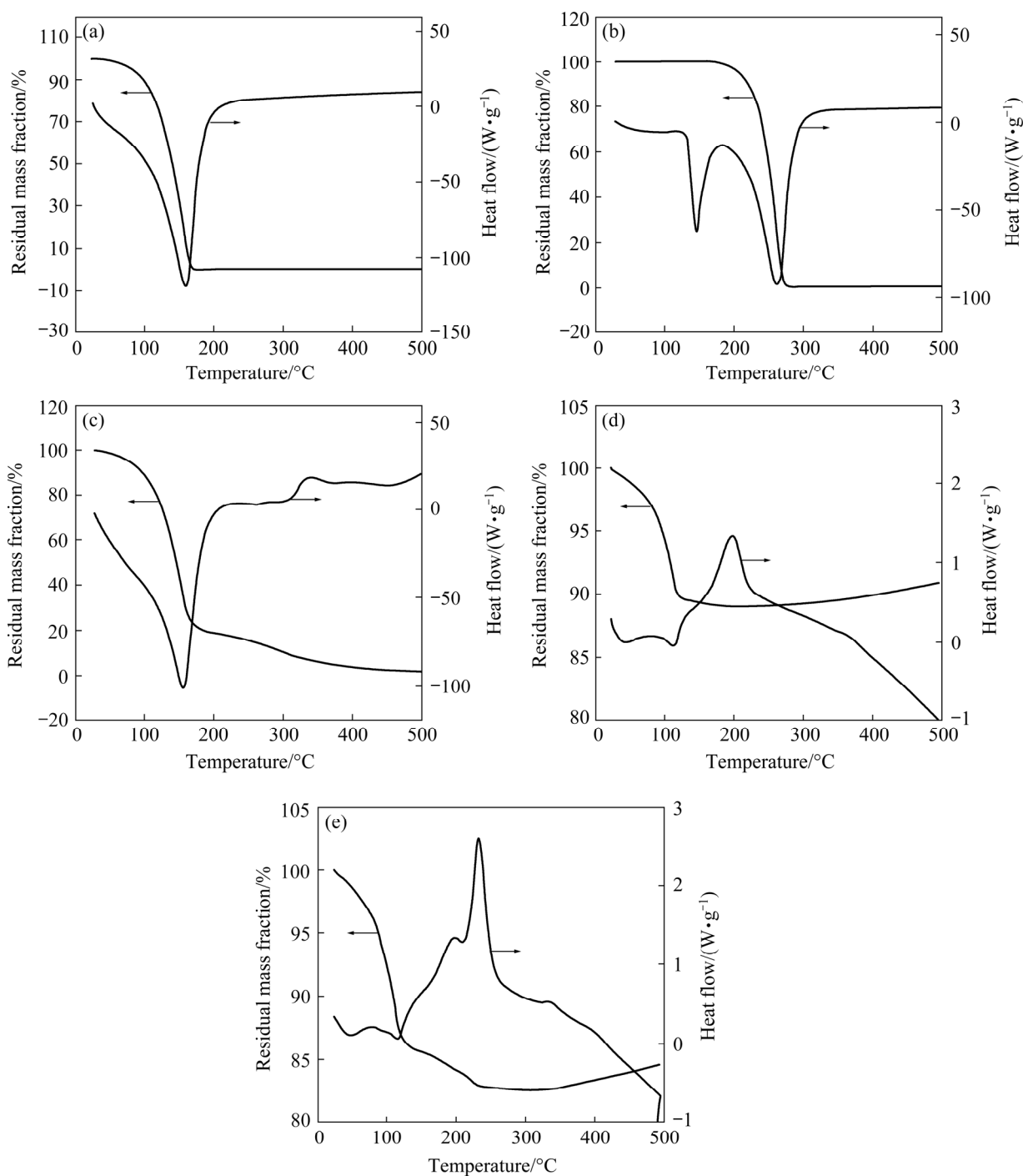


Fig. 3 TG–DTA curves of EG (a), MA (b), EG–20wt.%MA mixture (c), paste containing only EG solvent (d) and paste containing both EG solvent and MA (e)

for the paste did not correspond to the start temperature of the mass increase; the indexed temperatures of 194 and 232 °C were much lower than 299 °C. Hence, it was inferred that the prevalence of exothermic peaks was due to the sintering of the Cu particles.

Although the exothermic peak of the EG paste is also estimated to be enlarged due to the sintering

of Cu particles, the total area of the exothermic peaks of the EG–20wt.%MA paste is much larger than that of the EG paste, indicating an intensive sintering reaction. Consequently, the addition of 20wt.% MA to the paste significantly promoted the sintering of Cu particles and considerably delayed Cu oxidation. The enhanced sintering behavior can be attributed to the reduction of

copper oxide in Cu particles by MA. If adequate pressure is applied during the actual sinter bonding under conditions similar to the TG–DTA conditions, oxidation at high temperatures will be suppressed due to the formation of a bulk structure by rapid densification.

3.4 Sintering mechanism

To readily observe the sintering behavior of Cu particles in the EG–20wt.%MA paste during heating in air, the pressureless sintering behavior of the paste printed on a glass substrate was investigated. Figure 4 shows the microstructures observed at different sintering temperatures, the microstructural schematic representations and XRD patterns of the sample heated up to 300 °C. The sintering of particles in the paste was not confirmed immediately after reaching 194 °C (Fig. 4(a)), and an image containing noise was formed due to electrical charging, implying that the particles were covered by organic matter. Considering the TG

results of various samples in Fig. 3, the paste heated to 194 °C will contain MA because the mass at the temperature in Fig. 3(e) did not reach the minimum. However, obvious sintering at the contacts between the particles was observed as the temperature increased to 230 °C (Fig. 4(b)). If adequate pressure is applied during sintering, the degree of sintering will increase markedly with an increase in both the number and area of the contacts. Lastly, in the paste heated to 300 °C (Fig. 4(c)), slightly intensified sintering at the contacts was observed, although the surface of the particles became rough, indicating that the surfaces were oxidized with the formation of the Cu_2O phase, as confirmed by the XRD pattern in Fig. 4(e). Although extensive sintering was not observed due to the pressureless condition, the sintering between particles will be significantly promoted; the formation of a densified structure will suppress the oxidation during the increase in temperature to 300 °C if the sintering proceeds under adequate pressure.

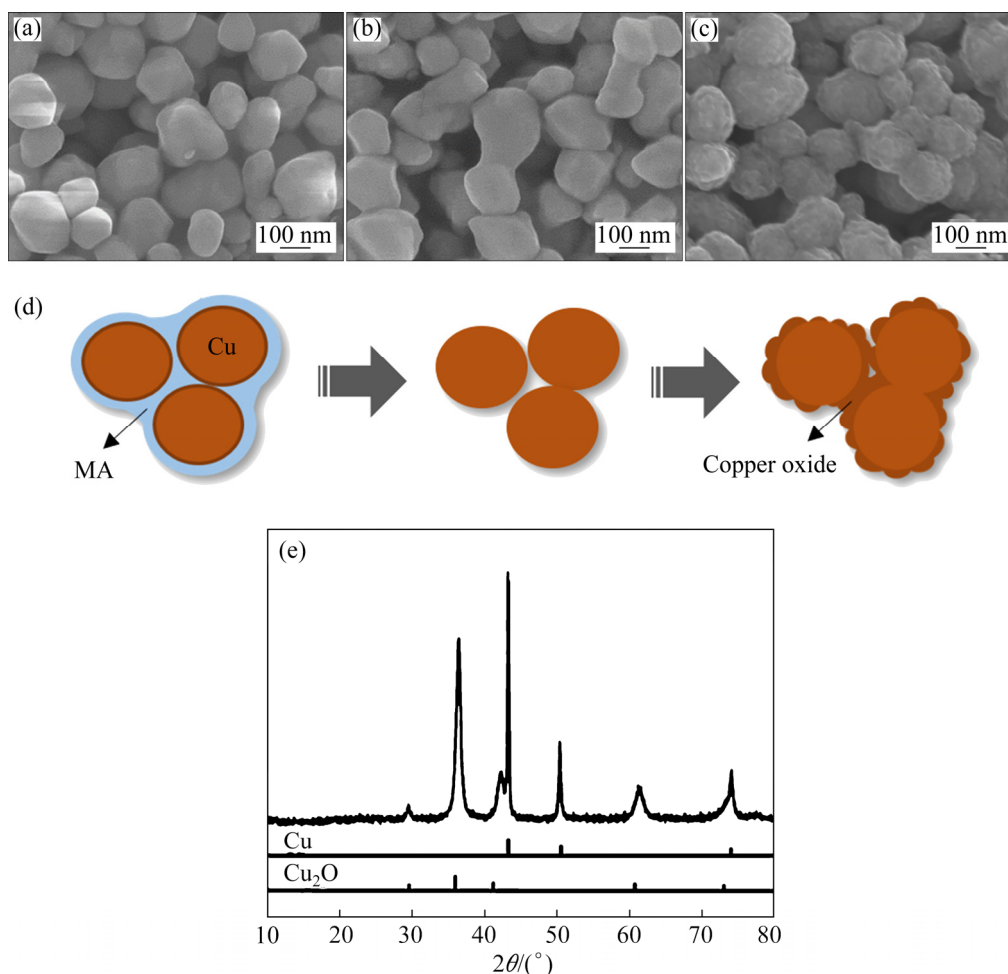


Fig. 4 SEM images (a–c), microstructural schematic representations (d) of printed EG–20wt.%MA paste observed after heating to 194 °C (a), 230 °C (b), and 300 °C (c), and XRD pattern of sample heated to 300 °C (e)

3.5 Shear strength of bondline

Figure 5 shows the measured shear strength as a function of the MA content for bondlines formed by the pressure (5 MPa)-assisted sinter bonding at 300 °C for 30 s, followed by pressureless annealing at 300 °C for 30 min. Without the addition of MA, the strength was 15.9 MPa. However, the shear strength increased proportionally with an increase in the MA content; the strengths were found to be 34.6 and 69.6 MPa, respectively, for the bondlines formed with the pastes containing 10 wt.% MA and 20 wt.% MA. These values are considerably higher than those of a bondline formed with the current high-Pb solder [16].

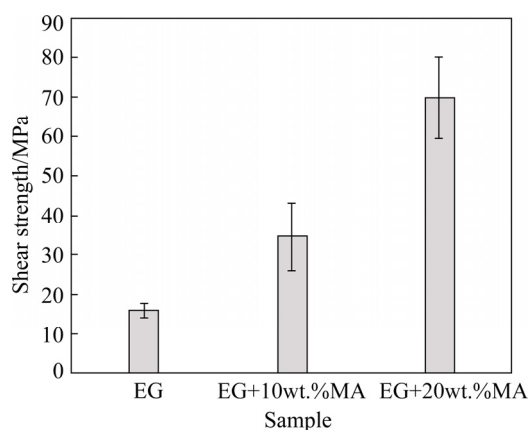


Fig. 5 Shear strength of bondlines with different MA contents (The bondlines were annealed at 300 °C for 30 min after sinter bonding under 5 MPa at 300 °C for 30 s)

To elucidate the effects of the pressure applied during sinter bonding and the annealing time on the shear strength of the bondline of the EG–20wt.%MA paste, the strength was measured for bondlines annealed at 300 °C for different time after sintering under 2 and 5 MPa at 300 °C for 30 s (Fig. 6). After sinter bonding under a pressure of 5 MPa, the strength increased significantly (from 23.1 MPa) with increasing annealing time. Accordingly, the strength increased up to 69.6 MPa after 30 min of annealing. All fractures occurred inside the bondlines. Although the strength may decrease slightly because of the oxidation of Cu particles and Cu finishes during aging in air, especially when the annealing time is long, the increase in the EG–20wt.%MA bondline is completely contrary to the reports on aging in air [17–19]. For the samples bonded under 2 MPa,

however, the strength did not increase with an increase in the annealing time. Thus, the annealing process was found to be effective for enhancing the bonding strength of the 5 MPa sample but not for the 2 MPa sample. The fracture location formed by shearing in all the 2 MPa samples moved to the interface between the bondline and the Cu substrate. The relatively low bondline density by 2 MPa compression induced oxidation on the Cu particles and Cu finishes during aging in air, resulting in an identical interface failure mode without an increase in shear strength. On the contrary, suppression of oxidation and a consistent increase in density are expected during the aging of the 5 MPa samples.

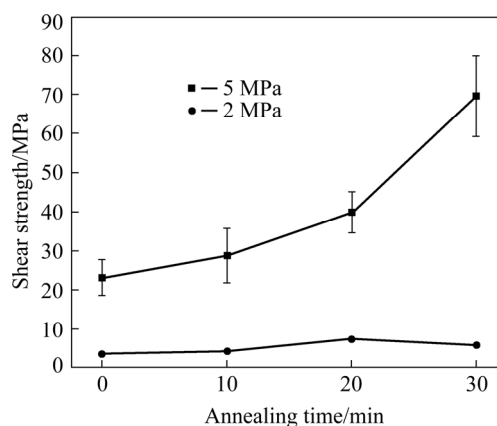


Fig. 6 Shear strength as function of annealing time at 300 °C after sinter bonding under 2 and 5 MPa at 300 °C for 30 s for EG–20wt.%MA paste

3.6 Microstructures of bondlines after annealing

The cross-sectional microstructures of the EG–20wt.%MA bondline after annealing are shown in Fig. 7. After the additional annealing process for 30 min, the microstructure of the bondline changed to a dense one, and a large number of voids between the particles transformed to grain boundaries. Accordingly, the measured porosity in Fig. 7(a) image decreased to 4.8%. Moreover, the sintered area between Cu particles and Cu finishes at the interfaces increased significantly. These microstructural changes account for the drastic increase in bonding strength after annealing. In addition, the high-density bondline formed by the EG–20wt.%MA paste could suppress the oxidation of Cu particles and Cu finishes during aging.

3.7 Fracture surfaces

SEM images of the fracture surfaces formed in the EG–20wt.%MA bondlines by the shear test

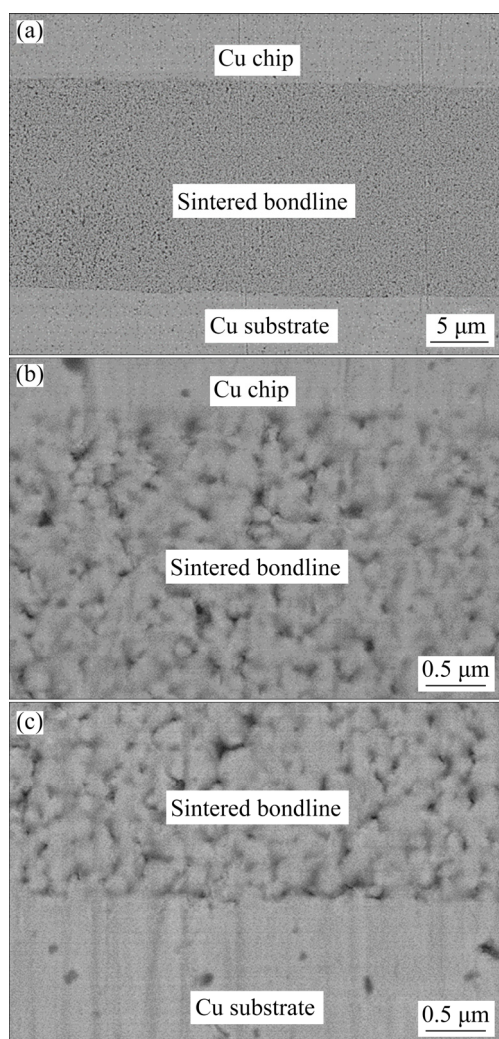


Fig. 7 Cross-sectional BSE images of bondlines obtained by additional annealing for 30 min after sinter bonding using EG–20wt.%MA paste: (a) Entire region; (b) Magnified upper interface region; (c) Magnified lower interface region

after the annealing treatment are displayed as a function of the annealing time (10–30 min) in Fig. 8. All the observed fractures were located inside the bondlines. In the fracture surface of the sample annealed for 10 min (Fig. 8(a)), the particulate surface and shear bands in the sintered regions were observed simultaneously, indicating insufficient particle sintering in the bondline. With an increase in the annealing time to 20 min (Fig. 8(b)), the area of the particulate surface decreased, whereas the area of the shear bands increased due to intensified sintering in the bondline. Eventually, the surfaces of the samples that were annealed for 30 min (Fig. 8(c)) were fully transformed to a ductile fracture mode (a regularly

elongated dimple microstructure with sharp tips) due to plastic deformation during the shearing process. The transition from a crumbly fracture to a ductile fracture indicates the trend of the shear strength enhancement with an increase in the annealing time.

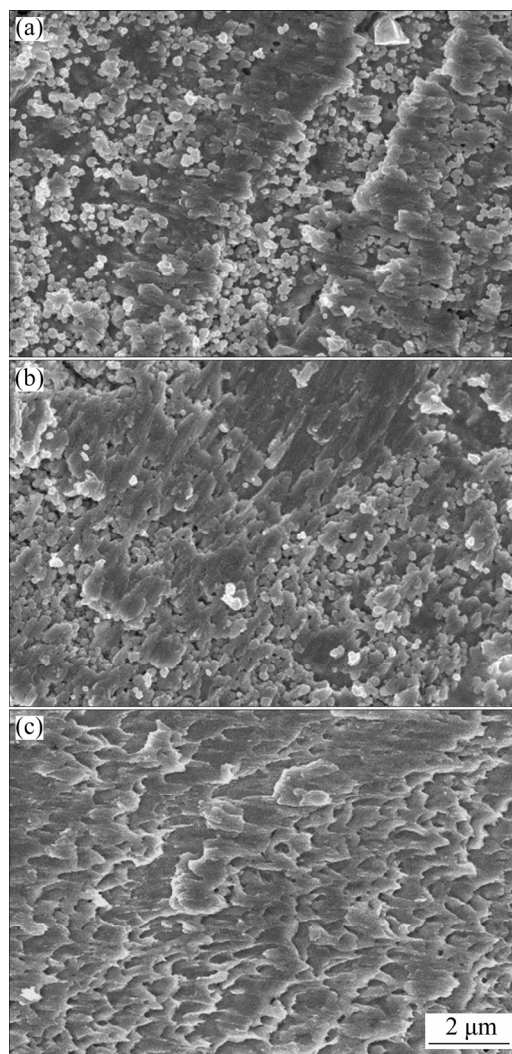


Fig. 8 SEM images of fracture surfaces for EG–20wt.%MA bondlines formed by shearing after annealing for different time: (a) 10 min; (b) 20 min; (c) 30 min

4 Conclusions

(1) With the addition of 20 wt.% MA to the EG solvent to reduce the copper oxide in Cu particles, the shear strength measured immediately after sinter bonding under 5 MPa at 300 °C for only 30 s was found to be 23.1 MPa.

(2) Successive annealing in a nitrogen atmosphere after adequate sinter bonding led to a significant increase in the strength with annealing

time. As a result, annealing for 30 min increased the strength up to 69.6 MPa. The fracture surface showed a ductile fracture mode caused by the tearing of the dense structure, indicating the achievement of tough bonding by the suggested process.

(3) The two-step sinter bonding process using low-cost Cu-particle-based paste is considered to be realistically applicable as a next-generation sinter bonding process of power devices and can provide an outstanding production rate.

Acknowledgments

This work was supported by the Materials & Components Technology Development Program (10080187) funded by the Ministry of Trade, Industry & Energy (MI, Korea).

References

- [1] HONG W S, KIM M S, HONG K K. Electrical and microstructural reliability of pressureless silver-sintered joints on silicon carbide power modules under thermal cycling and high-temperature storage [J]. *Journal of Electronic Materials*, 2021, 50: 914–925.
- [2] LEE Y J, LEE J H. Die sinter bonding in air using copper formate preform for formation of full-density bondline [J]. *Transactions of Nonferrous Metals Society of China*, 2021, 31: 1717–1728.
- [3] WANG M Y, MEI Y H, LI X, BURGOS R, BOROYEVICH D, LU G Q. How to determine surface roughness of copper substrate for robust pressureless sintered silver in air [J]. *Materials Letters*, 2018, 228: 327–330.
- [4] PENG Y, MOU Y, LIU J X, CHEN M X. Fabrication of high-strength Cu–Cu joint by low-temperature sintering micron-nano Cu composite paste [J]. *Journal of Materials Science: Materials in Electronics*, 2020, 31: 8456–8463.
- [5] CHEN W C, CHENG J G, CHEN H P, YE N M, WEI B Z, LUO L M, WU Y C. Nanosized copper powders prepared by gel-casting method and their application in lubricating oil [J]. *Transactions of Nonferrous Metals Society of China*, 2018, 28: 1186–1191.
- [6] ZUO Y, CARTER-SEARJEANT S, GREEN M, MILLS L, MANNAN S H. High bond strength Cu joints fabricated by rapid and pressureless in situ reduction-sintering of Cu nanoparticles [J]. *Materials Letters*, 2020, 276: 128260.
- [7] ISHIZAKI T, WATANABE R. A new one-pot method for the synthesis of Cu nanoparticles for low temperature bonding [J]. *Journal of Materials Chemistry*, 2012, 22: 25198–25206.
- [8] LIU J D, CHEN H T, JI H J, LI M Y. Highly conductive Cu–Cu joint formation by low-temperature sintering of formic acid-treated Cu nanoparticles [J]. *ACS Applied Materials & Interfaces*, 2016, 8: 33289–33298.
- [9] GAO Y, ZHANG H, LI W L, JIU J T, NAGAO S, SUGAHARA T, SUGANUM A K. Die bonding performance using bimodal Cu particle paste under different sintering atmospheres [J]. *Journal of Electronic Materials*, 2017, 46: 4575–4581.
- [10] MOU Y, LIU J X, CHENG H, PENG Y, CHEN M X. Facile preparation of self-reducible Cu nanoparticle paste for low temperature Cu–Cu bonding [J]. *JOM*, 2019, 71: 3076–3083.
- [11] ZUO Y, SHEN J, XIE J C, XIANG L. Influence of Cu micro/nano-particles mixture and surface roughness on the shear strength of Cu–Cu joints [J]. *Journal of Materials Processing Technology*, 2018, 257: 250–256.
- [12] MOU Y, CHENG H, PENG Y, CHEN M X. Fabrication of reliable Cu–Cu joints by low temperature bonding isopropanol stabilized Cu nanoparticles in air [J]. *Materials Letters*, 2018, 229: 353–356.
- [13] GAO Y, LI W L, CHEN C T, ZHANG H, JIU J T, LI C F, NAGAO S, SUGANUMA K. Novel copper particle paste with self-reduction and self-protection characteristics for die attachment of power semiconductor under a nitrogen atmosphere [J]. *Materials & Design*, 2018, 160: 1265–1272.
- [14] KANZAKI M, KAWAGUCHI Y, KAWASAKI H. Fabrication of conductive copper films on flexible polymer substrates by low-temperature sintering of composite Cu ink in air [J]. *ACS Applied Materials & Interfaces*, 2017, 9: 20852–20858.
- [15] MOU Y, PENG Y, ZHANG Y R, CHENG H, CHEN M X. Cu–Cu bonding enhancement at low temperature by using carboxylic acid surface-modified Cu nanoparticles [J]. *Materials Letters*, 2018, 227: 179–183.
- [16] SUGANUMA K, KIM S J, KIM K S. High-temperature lead-free solders: Properties and possibilities [J]. *JOM*, 2009, 61: 64–71.
- [17] KOGA S, NISHIKAWA H, SAITO M, MIZUNO J. Fabrication of nanoporous Cu sheet and application to bonding for high temperature applications [J]. *Journal of Electronic Materials*, 2020, 49: 2151–2158.
- [18] XIE J C, SHEN J, DENG J Z, CHEN X. Influence of aging atmosphere on the thermal stability of low-temperature rapidly sintered Cu nanoparticle paste joint [J]. *Journal of Electronic Materials*, 2020, 49: 2669–2676.
- [19] CHEN T F, SIOW K S. Comparing the mechanical and thermal-electrical properties of sintered copper (Cu) and sintered silver (Ag) joints [J]. *Journal of alloys and Compounds*, 2021, 866: 158783.

用 200 nm 铜颗粒在空气中快速压力辅助烧结及连续无压退火提高结合强度

Myeong In KIM, Jong-Hyun LEE

Department of Materials Science and Engineering, Seoul National University of Science and Technology,
232 Gongneung-ro, Nowon-gu, Seoul 139-743, Korea

摘 要: 为了设计一种有效且适用于功率器件的烧结结合工艺, 提出一种两步工艺, 使用约 200 nm 的铜颗粒基浆料形成具有高温可持续性和优越导热性的粘结层。该工艺涉及在空气中快速压力辅助烧结和在氮气气氛中连续无压退火。当使用 20%(质量分数)的羟基丁二酸和 80%(质量分数)的乙二醇混合物浆料时, 在 300 °C、5 MPa 烧结 30 s 后的剪切强度为 23.1 MPa。辅助无压烧结 30 min 后, 剪切强度显著提高至 69.6 MPa。因此, 两步烧结结合工艺有望作为下一代烧结结合工艺具有极高的生产效率。

关键词: 亚微米铜颗粒; 铜浆料; 羟基丁二酸; 烧结结合; 连续退火; 剪切强度

(Edited by Wei-ping CHEN)